Electronic Sensitivity of Carbon Nanotubes to Internal Water Wetting

Di Cao,[†,‡] Pei Pang,[†,‡] Jin He,[‡,*] Tao Luo,[†,‡] Jae Hyun Park,[⊥] Predrag Krstic,[⊥] Colin Nuckolls,[∥] Jinyao Tang,[∥] and Stuart Lindsay[†,‡,§,*]

[†]Department of Physics, [‡]Biodesign Institute, and [§]Department of Chemistry and Biochemistry, Arizona State University, Tempe, Arizona 85287, United States, [⊥]Physics Division, Oak Ridge National Laboratory, Oak Ridge, Tennessee 37831, United States, and [∥]Department of Chemistry, Columbia University, New York, New York 10027, United States

ABSTRACT We have constructed devices in which the interior of a single-walled carbon nanotube (SWCNT) field-effect transistor acts as a nanofluidic channel that connects two fluid reservoirs, permitting measurement of the electronic properties of the SWCNT as it is wetted by an analyte. Wetting of the inside of the SWCNT by water turns the transistor on, while wetting of the outside has little effect. These observations are consistent with theoretical simulations that show that internal water both generates a large dipole electric field, causing charge polarization of the tube and metal electrodes, and shifts the valence band of the SWCNT, while external water has little effect. This finding may provide a new method to investigate water behavior at nanoscale. This also opens a new avenue for building sensors in which the SWCNT simultaneously functions as a concentrator, nanopore, and extremely sensitive electronic detector, exploiting the enhanced sensitivity of the interior surface.

KEYWORDS: nanofluidics · nanopore · carbon nanotube · biosensor · nanoconfinement · water in nanoscale channels

The excellent electronic properties, small pore size, and large surface to volume ratio of single-walled carbon nanotubes (SWCNTs) form the basis of a large number of new types of electronic sensors[1−3] in which analytes generate a signal by binding to the outside of a SWCNT. However, the interior of the SWCNT is unexplored territory for chemical and biological sensor applications. Here, we address the question of how *internal* water wetting affects the electronic properties of the SWCNT (and the properties of the contacts to it).

Counterintuitively, the hydrophobic interior of SWCNTs is readily wetted because the surface tension of water is much lower than the threshold value.[4,5] Microscopically, the chemical potential of water is lower inside the SWCNT than in the bulk,[6] and water can be transported at many thousand times the speed possible with classical Poiseulle flow.[6−9] Internal wetting of CNTs has been verified by transmission electron microscopy (TEM)[10] and a number of spectroscopy methods,[11−15] showing that water is ordered inside a CNT. The transport of water, ions, and small molecules through CNTs has also been studied experimentally using membranes consisting of billions of carbon nanotubes in parallel.[7,8,16] Recently, we reported studies of ion and DNA translocation through individual SWCNTs[17] by making devices in which just one SWCNT connects two fluid reservoirs. Ionic currents were found to be much larger than predicted by a standard electrophoresis model, and DNA translocation was accompanied by electrical signals that differed drastically from what is observed in other inorganic nanopores.[18−20] A very recent study showed yet another (proton dominated) mode of transport in very long SWCNTs.[11]

SWCNT field-effect transistors (FETs) show that the electronic properties of SWCNTs are sensitive to their diameter, chirality, defects, doping,[21] adsorbates,[22,23] and environment,[2] though these effects can be masked by the dominant role of Schottky barriers at the metal−SWCNT junction.[24,25] Wetting of the outside of SWCNT-FETs by water changes their hysteresis and shifts their threshold gate voltage (V_{th}).[26−29] The resistivity of SWCNT mats falls when they are wetted (possibly both inside and outside),[13,30] but these results are difficult to interpret in terms of the response of individual SWCNTs. Thus, we have used our new devices, in which just one SWCNT connects two fluid reservoirs to compare the effects of external and internal wetting on SWCNT-FETs.

RESULTS AND DISCUSSION

The combined nanofluidic CNT-FET is shown in Figure 1. It consists of a single SWCNT that connects two fluid reservoirs formed in a PMMA resist using e-beam lithography. Source and drain electrodes are evaporated onto the SWCNT under the barrier,[31,32] and a heavily doped p-type silicon substrate acts as a backgate. Only

* Address correspondence to jinhe@asu.edu, stuart.lindsay@asu.edu.

Received for review January 20, 2011 and accepted March 28, 2011.

Published online March 31, 2011
10.1021/nn200251z

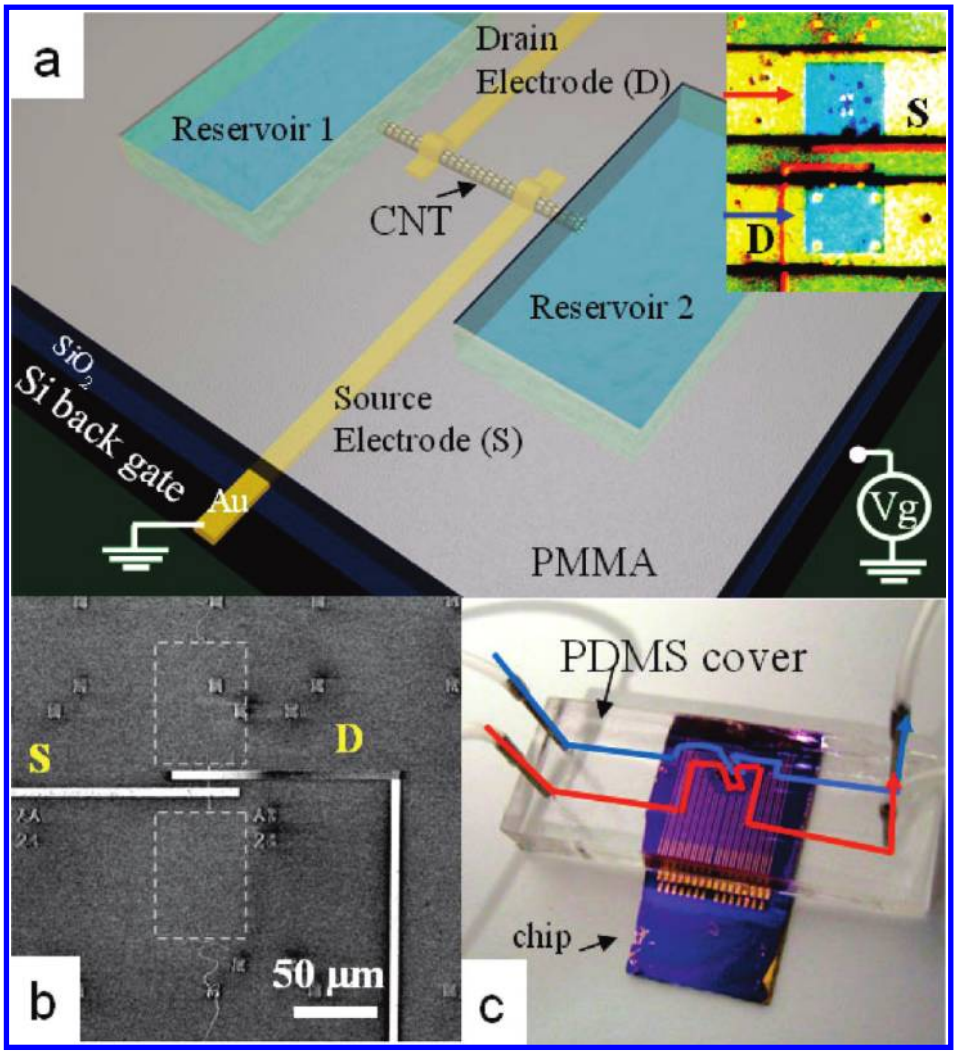

Figure 1. Measurement of a SWCNT nanofluidic channel integrated with a SWCNT field-effect transistor. (a) Schematic of the device structure and electrical measurement configuration. The inset shows an optical image of a device. The two blue squares (*i.e.*, 60 μm $\times$ 60 μm) are the fluid reservoirs cut into the PMMA (yellow). Areas contacted by the PDMS cover are shown in green. Fluid flow in the PDMS channels is indicated by the red and blue arrows. The distance between source (S) and drain (D) electrodes (red) is 15 μm. (b) Scanning electron microscopy (SEM) image of a single reservoir device after stripping off the PMMA layer to show the SWCNT lying under the electrodes. The areas labeled by the gray dashed squares indicate the position of the reservoirs. (c) Optical image of a device assembled with a PDMS cover for solution delivery. The red and blue lines show the fluid paths.

the SWCNT under the barrier remains after the exposed SWCNT in the reservoirs has been etched with an oxygen plasma.[17] The fluidic path is completed by attaching a PDMS cover containing microfluidic channels. Further details of the fabrication are given in the Methods.

We first characterized individual p-type semiconducting CNT-FETs prior to opening the SWCNT, both dry and with the exposed SWCNT wetted. We then opened the SWCNTs and recorded FET characteristics with the tube dry and wet. Only internal wetting had a significant effect on the characteristics of the device. Furthermore, vacuum drying of the SWCNT restored the prewetting characteristics. For controls, we (a) exposed the SWCNT between source and drain electrodes and wetted the tube externally in this region; (b) connected an electrode to the fluid reservoir and altered its potential (the extent possible with pure water); (c) varied the degree of plasma treatment of the reservoirs to alter surface charge in the reservoirs (Supporting Information Figure S3e). None of these controls altered the response of the SWCNT significantly. Thus, we conclude that water on the inside of the tube affects the contacts (and probably the band structure) of the tube in a way that water on the outside of the tube does not.

Representative data for one tube before opening are shown in Figure 2a. The source–drain current (I_{DS}) *versus* backgate voltage (V_{GS}) curves are for the dry tube in air (black curves) and for the tube externally wetted in the reservoir area (red curves). We observe an increase of hysteresis and a shift of the threshold gate

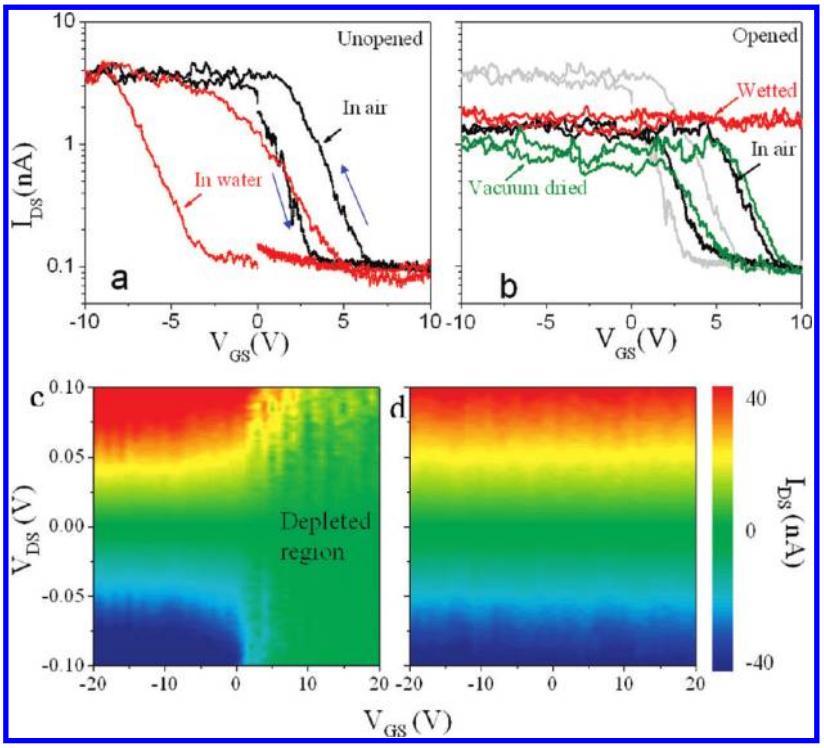

Figure 2. Effects of wetting on electronic transport in a SWCNT. (a) External wetting: $I_{DS}-V_{GS}$ semilog curves for an unopened p-type SWCNT device before (black) and after (red) filling the reservoirs with water at V_{DS} = 0.5 V. The blue arrows indicate the direction of the V_{GS} sweep. (b) Internal wetting: $I_{DS}-V_{GS}$ curves (V_{DS} = 0.5 V) before opening (gray), after opening with an oxygen plasma (black), after water is added to the reservoirs (red), and after the tube is subsequently dried in vacuum (green). (c) Heat map of I_{DS} (green = zero current) as a function of V_{GS} and V_{DS} for an unopened p-type SWCNT-FET. (d) Same as in c but internally wetted. The SWCNT is now ohmic over the entire range of V_{GS} and V_{DS}.

voltage (V_{th}) as reported earlier for external wetting.[26−29] Immediately after a gentle (~30 s, 7.2 W) oxygen plasma treatment to open the SWCNT (Figure 2b), we find that I_{DS} decreases a little in the saturation current region and V_{th} shifts slightly (black curve, Figure 2b). The characteristics change dramatically a few minutes after injection of water into the reservoir to wet the interior surface of the tubes (red curve, Figure 2b). The backgate bias no longer has any effect over the range of bias we can apply without breakdown. The transition is independent of drain−source bias as shown in heat maps (Figure 2c,d) of I_{DS} as a function of both V_{DS} and V_{GS}. Transistor action in the dry device (Figure 2c) is abolished over the entire range of V_{DS} and V_{GS} when it is wetted internally (Figure 2d). Furthermore, the effect is quite reversible: vacuum drying restores the function of the backgate (gray curve). Note that the "on" conductance of the tube does not change dramatically when the tube is internally wetted, the main effect being abolition of the action of the backgate.

When a p-type SWCNT-FET (keeping the electrodes protected) is externally wetted, its threshold moves toward more negative gate bias and hysteresis increases.[26−29] Internal wetting produces exactly the opposite result (Supporting Information Figure S1): the threshold moves to more positive gate bias and the hysteresis decreases.

Internal wetting abolished gating reversibly in 11 out of 18 measured semiconducting CNT devices and diminished it in 3 of the remaining 7 devices (Supporting Information Figure S5). Thus, the observation is not a result for a specific chirality or diameter, but a rather general property of single-walled semiconducting carbon nanotubes. We also measured three metallic CNT devices, and all showed *decreased* conductance after water filling (Supporting Information Figure S6).

We have ruled out some trivial causes for this effect. It is not a consequence of a short circuit between drain and source caused by external wetting. No amount of exposure to water alters the p-type FET response unless the SWCNTs are opened. We can also rule out the possibility that oxygen plasma treatment alters the tube in some way. Freshly opened tubes that are not exposed to water show p-type transistor action with characteristics only a little different from those measured prior to opening the tubes (black curves, Figure 2b). Another possibility is that the surface charges in the water reservoirs generated by oxygen plasma treatment may "pin" the potential of the CNT (through the poorly conducting medium of the water) out of the range of the backgate potential. We therefore measured the effect of sweeping the potential of a quasi-reference electrode (Pt wire) in contact with the water (water-gate, "V_{wg}" in Supporting Information Figure S3). This reference electrode plays the role of

introducing a strongly charged surface into the reservoir. The electronic transport characteristics of the CNT-FET device (with both unopened and opened CNT) were not sensitive (Supporting Information Figure S3) to the potential applied to the "water-gate" potential over a range of three volts, a potential change much larger than could be produced by any reasonable change in surface charge. Thus we can conclude that surface charges in contact with the water reservoir do not play an important role in our device. The most likely explanation for this is the high resistivity of (reasonably) pure water. Thus the potential of water inside the tube will be dictated by interactions with the tube, unless salt is added to the reservoirs.[2]

Studies of external wetting[26−29] have been carried out using a window opened in dielectric material that covers the metallic contacts (Supporting Information Figure S2). The difference between internal and external wetting may just reflect the fact that the tube is not wetted all the way up to the contact in the external wetting process. To check for this, we opened a window that exposed the electrodes as well, having first established that current flow through the water in contact with the electrodes is negligible (Supporting Information Figure S4a). External wetting of the tube all the way up to the contacts did move the threshold to more positive gate bias but did not result in abolition of gating (Supporting Information Figure S4b). So this difference between external and internal wetting does not account for the effects of internal wetting.

Finally, we considered the possibility that the gate field is modified by the dielectric properties of confined water[33] which will alter the capacitance of the tube, and hence its potential at a given gate bias, but estimates of this effect show that it is very small. Thus, we conclude that internal wetting must alter the electronic properties of the SWCNT and/or the Schottky barriers[25] at the contacts in a way that external wetting does not.

In order to investigate these effects further, we carried out molecular dynamics and electronic structure calculations for water confined inside a SWCNT. Turning first to water structures inside the tube, we filled a 2.84 nm long semiconducting (10,0) tube (0.78 nm diameter) with water and equilibrated the structure (see the Methods and Supporting Information for details). The resulting water structure is a single-file hydrogen-bonded "wire" (Supporting Information Figure S8). The dipole orientation of such water structure and the importance of the dipole orientation to the water transport through CNT have been studied before.[34,35] According to our estimates, the dipole field of this water structure is in magnitude competitive or even stronger than the electrical field of the backgate in both axial and radial components. This dipole field causes redistribution of the charges at the CNT and contact electrodes which cancel the dipole field but

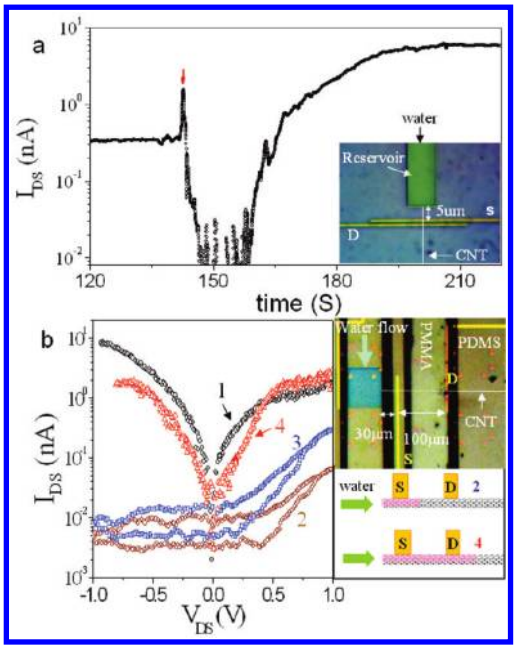

Figure 3. Change of electronic properties during wetting. (a) I_{DS} *vs* time for V_{GS} = 20 V and V_{DS} = 2 V. The red arrow marks the point of water addition, with current initially falling before rising to the equilibrium value. The optical microscopy image of the single reservoir device used for this measurement is shown in the inset. (b) $I_{DS}-V_{DS}$ curves (V_{GS} = 0 V) for a slow-filling device (inset top right) showing a transition from symmetric behavior (1) to rectification (2,3) and back to symmetric behavior (4) as the internal water propagates into the structure (inset bottom right).

also influences the electronic characteristics of the tube, including Schottky barriers. The water dipole will flip frequently,[36] but the flipping can be suppressed by the drain−source field. In contrast, external water generates essentially no dipole field. Thus internal water may generate an electric field and polarizes the tube and metal electrodes that modify the Schottky barrier at the contacts. These effects are not seen at external wetting.

Second, internal water may also modify the electronic structure of CNT, as suggested by the IR spectroscopy.[14] We have carried out DFT electronic structure calculations using the same CNT (10,0) tube. The CNT was filled with optimized and thermally equilibrated (300 K) water structure (Supporting Information Figure S12), using molecular dynamics simulations as discussed in the previous paragraph. A decrease in the band gap was observed when water molecules fully fill the CNT (red curve in Supporting Information Figure S12c).The CNT band gap decreases with the number of water molecules (Supporting Information Figure S13). The band gap is also reduced when water molecules are placed outside the tube. However, the decrease is much smaller (∼15%) even when a large number (115) of external water molecules were used. The reduction in the band gap of CNT originated from the enhanced interaction between ordered structure of water molecules and the carbon

atoms. Significantly stronger interaction is observed when water molecules are confined inside the tube (insets in Supporting Information Figure S12c), leading to a penetration of the occupied levels of oxygen into the CNT band gap. No shift in the CNT Fermi level was observed, and there was no charge transfer between internal water molecules and carbons. The CNT band gap reduction will lower the Schottky barriers and push V_{th} to a larger positive value.

On the basis of these simulations, it is clear that internal wetting can modify the electronic property of device either through dipole electric field and induced polarizations mediated modification of the Schottky barriers and/or *via* the shift of the valence band owing to the band gap reduction. We devised an experiment to separate the effects of internal wetting on the contacts from the effects on the electronic properties of the tube itself. To do this, we opened the SWCNT at one end only, so that the internal wetting would proceed slowly, passing first one contact, then the interior of the device, and finally the second contact, measuring the current through the device as the wetting proceeded. Figure 3a shows a typical current *versus* time trace for a device gated partially "on" initially. Interestingly, the current first *drops* and then rises to the saturated "on" value (note the current scale is logarithmic). Since, as revealed by Supporting Information Figure S13a and quantum calculations, the internal wetting has a minimal effect on the valence band when the wetting is less than 25% of one side and becomes really significant at more than 75% of the tube filling, this result implies that wetting *increases* the Schottky barrier at the first contact, an effect that is eventually counteracted by the upward movement of the valence band. It was shown previously that asymmetric Schottky barriers (generated by different metal contacts[37] or an extra gate near one contact[38]) will produce rectifying behavior. We slowed down the wetting process by using a tube with a 100 μm separation between the source and drain electrodes so that we could record I_{DS} as a function of V_{DS} as wetting proceeded (the backgate was set to turn the device "on" initially). Initially (1 in Figure 3b) the $I_{DS}-V_{DS}$ curve was symmetric. However, at intermediate times (2 and 3 in Figure 3b), the device showed rectification, returning to a symmetric response (4 in Figure 3b) as both contacts became wetted.

We can qualitatively account for our observations by assuming (a) that the Schottky barriers are first increased due to the water dipole induced polarizations of the CNT and metal electrodes, in particular, as predicted by the molecular dynamics simulations and (b) that the valence band is then shifted upward (narrowing the Schottky barriers) as predicted by the DFT calculations. Figure 4a shows the device switched "on" (blue dashed lines) at $V_{GS} = 0$ and "off" (orange dashed lines) at $V_{GS} > 0$ when the tube is dry. When

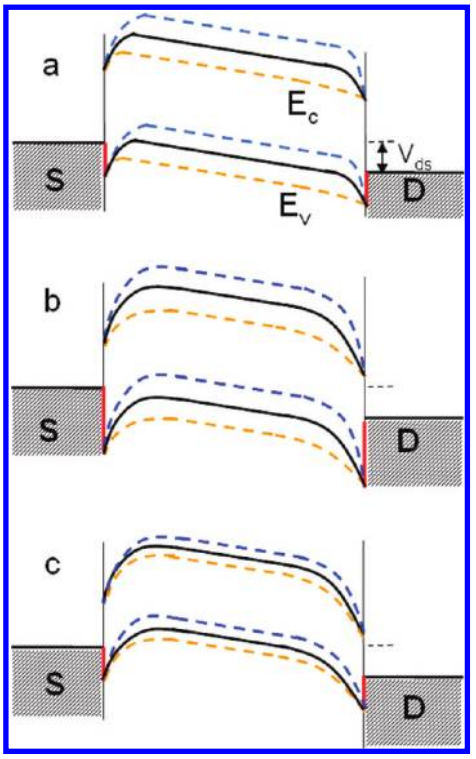

Figure 4. Sequential change of the energy band diagrams of a CNT-FET device during water wetting process at a fixed positive V_{DS} and different V_{GS} (orange, positive; black, zero; blue, negative). (a) Initial diagram before wetting. (b) Increase of Schottky barrier at contacts. (c) Upshift of valence band (E_V) while the CNT Fermi level is fixed. The red lines indicate the heights of Schottky barriers. S and D are source and drain electrodes, respectively. In the diagrams, the contact resistance is neglected and the Fermi level between metal contact and CNT is always in alignment.

water wets the inside of the CNT under the first contact, an increase of the Schottky barrier height (Figure 4b) leads to a current (I_{DS}) drop. With the further wetting of the CNT interior, the upward shift of valence band (E_V) (Figure 4c) lowers the Schottky barrier height, turning the device on. A significant shift in E_V and/or a large local polarization field at contacts (due to the induced image charges at electrodes from the polarized CNT) will overcome the ability of the backgate to modulate the conductance (indicated schematically by the smaller difference between the dashed orange and blue lines in Figure 4c) and also turns the device "on" at $V_{GS} > 0$. We often observed a similar or slightly smaller "on" conductance of the devices after water wetting, which implies a similar Schottky barrier or a large metal–CNT contact resistance.

Internal wetting with a salt solutions (0.1 mM KCl) immediately restored p-type transistor action in tubes that had been rendered insensitive to gating by pure water (Supporting Information Figure S7). The change may be due to the disruption of the ordered water structure and the water–CNT interaction inside the CNT by the hydrated salt ions. At 0.1 mM salt, a 15 μm long SWCNT contains approximately 3 K^+ and 3 Cl^-

ions and 10^6 water molecules, so water ordering would have to be extremely sensitive to the presence of just a few ions. A second possibility is that the carbon nanotube potential needs to float with respect to the reservoirs for the abolition of gating to be observed. The addition of salt will add the capacitance of all of the electrolyte in the reservoir to that of the tube, effectively pinning the tube potential.

In summary, we have studied electronic transport in individual SWCNTs as they are filled by water. The tubes are extremely sensitive to internal wetting, which affects the CNT potential and band gap structure, owing to the nanoconfinement of water. Thus this work provides a new method to investigate water at nanoscale. Furthermore, SWCNTs are likely to be even more sensitive to internal analytes than they are to external analytes. Using the inside of the tube as the sensing surface will also permit the SWCNT to be used as a nanopore (for analyzing single molecules[17]) and as a nanoscale sample concentrator because of the ion selectivity of SWCNTs[39,40] and the enhanced water flow inside them.[7,8] Analytes dissolved in water that enter the CNT slowly will accumulate owing to the several-thousand-fold enhancement of water flux through the tube.

METHODS

Device Fabrication. We first grew well-separated single-walled carbon nanotubes (SWCNTs) on boron-doped silicon wafers (used as a backgate) with 1000 nm of thermal oxide. Cobalt nanoparticles were used as catalyst, and the carbon source was ethanol vapor. Conditions were chosen to produce high-quality SWCNTs with an outside diameter of 1−2 nm.[17] Gold markers and large electrical pads were fabricated using optical lithography. SEM images were used to locate the SWCNTs' position relative to the markers. After SEM imaging, the chips were heated at 400 °C in air for 1 h to remove resist residue. Immediately after cleaning, the Au/Cr metal electrodes for contacting the SWCNTs (normally 5 μm in width and 40 nm/5 nm in thickness) were fabricated using electron-beam lithography (EBL) and the electrical properties of SWCNT were measured in ambient air. SWCNTs with good electrical properties were selected for the next step. We then spun-on a 900 nm thick layer of poly(methyl methacrylate) (PMMA, A8) over the entire device structure, and wells were formed along the path of a SWCNT using EBL aligned relative to the markers.

Electrical Measurements. The electrical measurements were carried out in a home-built probe station inside a faraday cage. A Keithley SourceMeter 2636A, a low noise current meter 6514, and a function generator (DS 345, Stanford research system) were used and controlled by custom labview programs.

Theory. The density functional theory (DFT) calculations were performed with the computational chemistry package NWChem[41] using 12 000 processors at the Cray XT5 computer (Jaguar) of the National Center of Computer Sciences (NCCS), ORNL. The molecular dynamics (MD) calculations were performed at the Cray XT5 computer (Kraken) of National Institute of Computational Sciences (NICS), UT Knoxville, using the computer package GROMACS.[42] Hydration geometries were determined using MD simulations on a (10,0) carbon nanotube of various lengths (2.84 nm, 280 C atoms, and 1.56 nm, 160 atoms), of 7.8 Å diameter, partially and fully filled with water, as well as wetted outside. Eleven water molecules filled the longer nanotube, forming a chain, while 115 water atoms wetted the CNT externally. We performed the all-electron calculations using the 3-21g (3s2p) basis and the GGA nonlocal hybrid DFT exchange-correlation functional, with Gaussian smearing of 0.13 eV in the case of the water filling and of 0.54 eV for the external wetting. Full details are given in the Supporting Information.

Acknowledgment. We thank H. Liu and W.S. Song for assistance in the lab. We also acknowledge the use of nanofabrication facilities within the Center for Solid State Science (CSSS) at Arizona State University. This work was supported by the DNA Sequencing Technology Program of the National Human Genome Research Institute (1RC2HG005625-01, 1R21HG004770-01), Arizona Technology Enterprises and the Biodesign Institute. This research used resources of the Oak Ridge Leadership Facility at the Oak Ridge National Laboratory, which is supported by the Office of Science of the U.S. Department of Energy under Contract No. DE-AC05-00OR22725.

Supporting Information Available: Transport characteristics of a device measured at different times during the water filling process, effect of external wetting with protected and exposed electrodes, water gating, tubes that did not show a full metallic transition, internal wetting of metallic tubes, effects of salt addition, and details of theory. This material is available free of charge *via* the Internet at http://pubs.acs.org.

REFERENCES AND NOTES

1. Kong, J.; Franklin, N. R.; Zhou, C.; Chapline, M. G.; Peng, S.; Cho, K.; Dai, H. Nanotube Molecular Wires as Chemical Sensors. *Science* **2000,** *287*, 622–625.
2. Douglas, R. K.; Alexander, S. Carbon Nanotube Gas and Vapor Sensors. *Angew. Chem., Int. Ed.* **2008,** *47*, 6550–6570.
3. Wenrong, Y.; Kyle, R.; Simon, R.; Pall, T.; Justin, G.; Filip, B. Carbon Nanomaterials in Biosensors: Should You Use Nanotubes or Graphene? *Angew. Chem., Int. Ed.* **2010,** *49*, 2114–2138.
4. Dujardin, E.; Ebbesen, T. W.; Hiura, H.; Tanigaki, K. Capillarity and Wetting of Carbon Nanotubes. *Science* **1994,** *265*, 1850–1852.
5. Erik, D.; Thomas, W. E.; Ajit, K.; Michael, M. J. T. Wetting of Single Shell Carbon Nanotubes. *Adv. Mater.* **1998,** *10*, 1472–1475.
6. Hummer, G.; Rasaiah, J. C.; Noworyta, J. P. Water Conduction through the Hydrophobic Channel of a Carbon Nanotube. *Nature* **2001,** *414*, 188–190.
7. Hinds, B. J.; Chopra, N.; Rantell, T.; Andrews, R.; Gavalas, V.; Bachas, L. G. Aligned Multiwalled Carbon Nanotube Membranes. *Science* **2004,** *303*, 62–65.
8. Holt, J. K.; Park, H. G.; Wang, Y. M.; Stadermann, M.; Artyukhin, A. B.; Grigoropoulos, C. P.; Noy, A.; Bakajin, O. Fast Mass Transport through Sub-2-Nanometer Carbon Nanotubes. *Science* **2006,** *312*, 1034–1037.
9. Joseph, S.; Aluru, N. R. Why Are Carbon Nanotubes Fast Transporters of Water? *Nano Lett.* **2008,** *8*, 452–458.
10. Naguib, N.; Ye, H.; Gogotsi, Y.; Yazicioglu, A. G.; Megaridis, C. M.; Yoshimura, M. Observation of Water Confined in Nanometer Channels of Closed Carbon Nanotubes. *Nano Lett.* **2004,** *4*, 2237–2243.
11. Cambreacute, S.; Schoeters, B.; Luyckx, S.; Goovaerts, E.; Wenseleers, W. Experimental Observation of Single-File Water Filling of Thin Single-Wall Carbon Nanotubes down to Chiral Index (5,3). *Phys. Rev. Lett.* **2010,** *104*, 207401.

12. Chen, Q.; Herberg, J. L.; Mogilevsky, G.; Wang, H.-J.; Stadermann, M.; Holt, J. K.; Wu, Y. Identification of Endohedral Water in Single-Walled Carbon Nanotubes by ^{1}H NMR. *Nano Lett.* **2008,** *8*, 1902–1905.
13. Maniwa, Y.; Matsuda, K.; Kyakuno, H.; Ogasawara, S.; Hibi, T.; Kadowaki, H.; Suzuki, S.; Achiba, Y.; Kataura, H. Water-Filled Single-Wall Carbon Nanotubes as Molecular Nanovalves. *Nat. Mater.* **2007,** *6*, 135–141.
14. Byl, O.; Liu, J.-C.; Wang, Y.; Yim, W.-L.; Johnson, J. K.; Yates, J. T. Unusual Hydrogen Bonding in Water-Filled Carbon Nanotubes. *J. Am. Chem. Soc.* **2006,** *128*, 12090–12097.
15. Kolesnikov, A. I.; Zanotti, J.-M.; Loong, C.-K.; Thiyagarajan, P.; Moravsky, A. P.; Loutfy, R. O.; Burnham, C. J. Anomalously Soft Dynamics of Water in a Nanotube: A Revelation of Nanoscale Confinement. *Phys. Rev. Lett.* **2004,** *93*, 035503.
16. Whitby, M.; Quirke, N. Fluid Flow in Carbon Nanotubes and Nanopipes. *Nat. Nanotechnol.* **2007,** *2*, 87–94.
17. Liu, H.; He, J.; Tang, J.; Liu, H.; Pang, P.; Cao, D.; Krstic, P.; Joseph, S.; Lindsay, S.; Nuckolls, C. Translocation of Single-Stranded DNA through Single-Walled Carbon Nanotubes. *Science* **2010,** *327*, 64–67.
18. Liang, X.; Chou, S. Y. Nanogap Detector Inside Nanofluidic Channel for Fast Real-Time Label-Free DNA Analysis. *Nano Lett.* **2008,** *8*, 1472–1476.
19. Dekker, C. Solid-State Nanopores. *Nat. Nanotechnol.* **2007,** *2*, 209–215.
20. Fan, R.; Karnik, R.; Yue, M.; Li, D.; Majumdar, A.; Yang, P. DNA Translocation in Inorganic Nanotubes. *Nano Lett.* **2005,** *5*, 1633–1637.
21. Lee, R. S.; Kim, H. J.; Fischer, J. E.; Thess, A.; Smalley, R. E. Conductivity Enhancement in Single-Walled Carbon Nanotube Bundles Doped with K and Br. *Nature* **1997,** *388*, 255–257.
22. Staii, C.; Johnson, A. T.; Chen, M.; Gelperin, A. DNA-Decorated Carbon Nanotubes for Chemical Sensing. *Nano Lett.* **2005,** *5*, 1774–1778.
23. Star, A.; Gabriel, J.-C. P.; Bradley, K.; Gruner, G. Electronic Detection of Specific Protein Binding Using Nanotube FET Devices. *Nano Lett.* **2003,** *3*, 459–463.
24. Heinze, S.; Tersoff, J.; Martel, R.; Derycke, V.; Appenzeller, J.; Avouris, P. Carbon Nanotubes as Schottky Barrier Transistors. *Phys. Rev. Lett.* **2002,** *89*, 106801.
25. Avouris, P.; Chen, Z.; Perebeinos, V. Carbon-Based Electronics. *Nat. Nanotechnol.* **2007,** *2*, 605–615.
26. Pati, R.; Zhang, Y.; Nayak, S. K.; Ajayan, P. M. Effect of H_2O Adsorption on Electron Transport in a Carbon Nanotube. *Appl. Phys. Lett.* **2002,** *81*, 2638–2640.
27. Na, P. S.; Kim, H.; So, H.-M.; Kong, K.-J.; Chang, H.; Ryu, B. H.; Choi, Y.; Lee, J. O.; Kim, B.-K.; Kim, J.-J.; *et al.* Investigation of the Humidity Effect on the Electrical Properties of Single-Walled Carbon Nanotube Transistors. *Appl. Phys. Lett.* **2005,** *87*, 093101.
28. Sung, D.; Hong, S.; Kim, Y.-H.; Park, N.; Kim, S.; Maeng, S. L.; Kim, K.-C. *Ab Initio* Study of the Effect of Water Adsorption on the Carbon Nanotube Field-Effect Transistor. *Appl. Phys. Lett.* **2006,** *89*, 243110.
29. Kim, W.; Javey, A.; Vermesh, O.; Wang, Q.; Li, Y.; Dai, H. Hysteresis Caused by Water Molecules in Carbon Nanotube Field-Effect Transistors. *Nano Lett.* **2003,** *3*, 193–198.
30. Zahab, A.; Spina, L.; Poncharal, P.; Marliere, C. Water-Vapor Effect on the Electrical Conductivity of a Single-Walled Carbon Nanotube Mat. *Phys. Rev. B* **2000,** *62*, 10000.
31. Heller, I.; Mannik, J.; Lemay, S. G.; Dekker, C. Optimizing the Signal-to-Noise Ratio for Biosensing with Carbon Nanotube Transistors. *Nano Lett.* **2009,** *9*, 377–382.
32. Cui, X.; Freitag, M.; Martel, R.; Brus, L.; Avouris, P. Controlling Energy-Level Alignments at Carbon Nanotube/Au Contacts. *Nano Lett.* **2003,** *3*, 783–787.
33. Bradley, K.; Cumings, J.; Star, A.; Gabriel, J.-C. P.; Gruner, G. Influence of Mobile Ions on Nanotube Based FET Devices. *Nano Lett.* **2003,** *3*, 639–641.
34. Zuo, G.; Shen, R.; Ma, S.; Guo, W. Transport Properties of Single-File Water Molecules Inside a Carbon Nanotube Biomimicking Water Channel. *ACS Nano* **2009,** *4*, 205–210.
35. Joseph, S.; Aluru, N. R. Pumping of Confined Water in Carbon Nanotubes by Rotation−Translation Coupling. *Phys. Rev. Lett.* **2008,** *101*, 064502.
36. Won, C. Y.; Joseph, S.; Aluru, N. R. Effect of Quantum Partial Charges on the Structure and Dynamics of Water in Single-Walled Carbon Nanotubes. *J. Chem. Phys.* **2006,** *125*, 114701.
37. Yang, M. H.; Teo, K. B. K.; Milne, W. I.; Hasko, D. G. Carbon Nanotube Schottky Diode and Directionally Dependent Field-Effect Transistor Using Asymmetrical Contacts. *Appl. Phys. Lett.* **2005,** *87*, 253116.
38. Marcus, F.; Marko, R.; Yangxin, Z.; Johnson, A. T.; Walter, F. S. Controlled Creation of a Carbon Nanotube Diode by a Scanned Gate. *Appl. Phys. Lett.* **2001,** *79*, 3326–3328.
39. Majumder, M.; Chopra, N.; Hinds, B. J. Effect of Tip Functionalization on Transport through Vertically Oriented Carbon Nanotube Membranes. *J. Am. Chem. Soc.* **2005,** *127*, 9062–9070.
40. Fornasiero, F.; Park, H. G.; Holt, J. K.; Stadermann, M.; Grigoropoulos, C. P.; Noy, A.; Bakajin, O. Ion Exclusion by Sub-2-nm Carbon Nanotube Pores. *Proc. Natl. Acad. Sci. U. S.A.* **2008,** *105*, 17250–17255.
41. Kendall, R. A.; Apr, E.; Bernholdt, D. E.; Bylaska, E. J.; Dupuis, M.; Fann, G. I.; Harrison, R. J.; Ju, J.; Nichols, J. A.; Nieplocha, J.; *et al.* High Performance Computational Chemistry: An Overview of NWChem a Distributed Parallel Application. *Comput. Phys. Commun.* **2000,** *128*, 260–283.
42. Biswas, P. K.; Gogonea, V. A Regularized and Renormalized Electrostatic Coupling Hamiltonian for Hybrid Quantum-Mechanical−Molecular-Mechanical Calculations. *J. Chem. Phys.* **2005,** *123*, 164114.